POSTER 8

Title:
Fluorescence guidance improves accuracy of radiological imaging-guided surgical navigation

This work was funded by the National Institutes of Health.

Author List:
Eric R. Henderson[1,2,3], Kendra A. Hebert[1], Samuel S. Streeter[1], Paul M. Werth[2,3], Eben L. Rosenthal[4], Keith D. Paulsen[1], Brian W. Pogue[5], Kimberley S. Samkoe[1]

[1]Thayer School of Engineering, Dartmouth College, Hanover, NH 03755.
[2]Geisel School of Medicine, Dartmouth College, Hanover, NH 03755.
[3]Department of Orthopaedics, Dartmouth-Hitchcock Medical Center, Lebanon, NH 03756.
[4]Department of Otolaryngology, Vanderbilt University Medical Center, Nashville, TN 37235.
[5]Department of Medical Physics, University of Wisconsin-Madison, Madison, WI 53706.

Background:
Imaging-based surgical navigation requires static referencing between the target anatomy and the imaging data provided to the clinical team. Imaging-based navigation is therefore well suited for operations involving relatively static features, such as bony anatomy. However, these technologies have not translated well to soft-tissue surgery due to an inability to adapt to positional changes during the procedure. STSs generally have poor responses to chemotherapy and modest responses to radiation; complete surgical excision of a non-metastatic primary tumor is therefore the only reliable curative treatment. STSs are optimally removed when the primary tumor is resected with a surrounding margin of normal, non-cancerous tissue through a surgical technique called a *wide local excision* (WLE).

Background:
In this project, fluorescence imaging, which provides dynamic and real-time tissue recognition, was evaluated in combination with conventional imaging-based navigation to guide WLE of validated STS phantom tumors. The hypothesis was that the best performance for WLE would be achieved with a combination of computed tomography (CT), magnetic resonance (MR), and/or fluorescence imaging technologies.

Background:
Semi-solid, gelatin-based human tissue-simulating phantoms were fabricated (14 cm in diameter, 11 cm in height), each with a cubical 'tumor' inclusion (8 cm^3) containing physiologically accurate concentrations of imaging contrast and fluorophore for an STS (Figure 1A-B). The phantom bulk material had either muscle- or adipose-mimicking optical properties. To facilitate CT- and MR-based navigation, each inclusion received a volume-equivalent human dose of 1.25 mL/kg of iohexol and 0.2 mL/kg of gadoterate, respectively. To facilitate fluorescence navigation, inclusions received scaled amounts of IRDye 800CW Carboxylate to obtain a 4:1 ratio relative to the phantom stroma, which replicated the adipose- and muscle-to-tumor ratios previously measured in human xenografts and *in vivo* human work for ABY-029. Ten phantoms each—five adipose-based and five muscle-based—were assigned to one of nine groups (90 phantoms total). Eight groups were assigned one or more navigation modalities; one group had no navigation or imaging (Figure 1C). Phantoms were dissected iteratively using all possible combinations of CT, MR, and fluorescence imaging, including control. Phantom groups were presented in random order, and the study dissector—a board-certified orthopaedic surgeon—was blinded to both the location and depth of the inclusions. Data collected were margin accuracy (mean deviation from goal margin of 1 cm, MΔ), margin status (positive or negative), spatial alignment of tumor inclusion with specimen (°), and dissection duration (min). Univariate and multivariate regression were utilized to explore the performance differences between combinations of imaging modalities.

Background:

Margin accuracy was higher for combined navigation modalities compared to individual navigation modalities, and accuracy was highest with combined CT and fluorescence navigation (MΔ = 1.9 mm, SD = 1.6 mm) as compared to any alternative single or combination of navigation technologies (Intercept = 4.87 mm, B = -2.83 mm, Student's t-test p = 0.045). Specimen-tumor alignment was also highest with combined CT and fluorescence navigation (M = 3.4°, SD = 3.5°) as compared to any alternative single or combination of navigation technologies (Intercept = 13.63°, B = -9.83°, Student's t-test p<0.001) and improved overall with combined navigation modalities.

Background:
At present, imaging-based navigation has limited application to guiding STS operations due to its inability to compensate for positional changes during surgery. This work indicates that fluorescence guidance enhances the accuracy of imaging-based navigation and may be best viewed as a synergistic technology, rather than a competing one.

Figure:

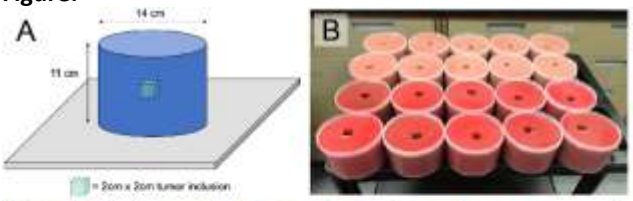

C

Table 1. Phantom imaging groups and respective applied imaging modalities

	Groups	1 n = 10	2 n = 10	3 n = 10	4 n = 10	5 n = 10	6 n = 10	7 n = 10	8 n = 10	9 n = 10
Navigation	CT		Yes		Yes		Yes		Yes	
	MRI			Yes	Yes			Yes	Yes	
	FGS					Yes	Yes	Yes	Yes	
Conventional MR and CT imaging		Yes				Yes				

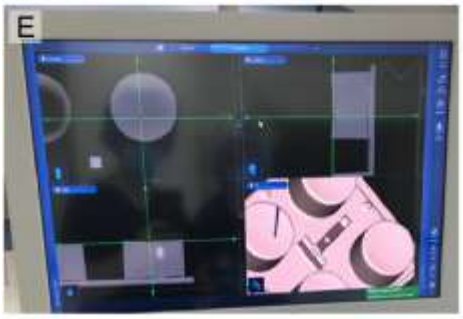

F

Results by group	Fluorescence (FGS)	CT - conventional	MRI - conventional	CT - navigation	MRI - navigation	Margin Accuracy: margin Δ (mm)	StdDev	Max	Min	WLE Result (+ / -)	Duration: Time (m:s)	Tumor-Specimen Alignment: (°)	StdDev	Max	Min
Group 0 (no imaging)	0	0	0	0	0	8.1	6.1	27.9	0.0	15	NA	23.3	12.8	44	4
Group 1	0	1	1	0	0	2.2	1.7	5.4	0.1	0	02:29	9.4	7.9	20	0
Group 2	0	0	0	1	0	3.4	2.6	9.0	0.0	0	04:52	6.4	5.4	15	1
Group 3	0	0	0	0	1	4.4	2.9	10.0	0.0	4	03:47	8.3	9.0	29	0
Group 4	0	0	0	1	1	3.1	2.8	13.1	0.1	1	04:32	3.7	3.9	10	0
Group 5	1	1	1	0	0	3.0	2.3	11.3	0.3	0	06:06	7.2	8.0	28	0
Group 6	1	0	0	1	0	1.9	1.5	5.2	0.0	0	07:35	3.4	3.5	9	0
Group 7	1	0	0	0	1	2.1	1.9	10.0	0.1	1	06:43	5.4	5.0	16	0
Group 8	1	0	0	1	1	2.0	1.9	10.0	0.1	1	06:56	4.2	3.7	10	0
fluorescence															
FGS - no	0					3.3	0.0	9.4	0.0	5	03:55	7.0	6.6	19	0
FGS - yes	1					2.2	0.0	10.0	0.1	2	06:50	6.4	6.6	21	0
All imaging-based navigation															
Navigation - no				0	0	2.6	0.0	8.4	0.2	0	04:17	8.3	8.0	24	0
Navigation - yes				1	1	2.8	0.0	9.6	0.0	7	05:44	5.2	5.1	15	0
CT imaging-based navigation															
CT navigation - no				0		2.9	0.0	9.2	0.1	5	04:46	7.6	7.5	23	0
CT navigation - yes				1		2.6	0.0	9.3	0.0	2	05:59	4.4	4.1	11	0
MR imaging-based navigation															
MR navigation - no					0	2.6	0.0	7.7	0.1	0	05:16	6.6	6.2	18	0
MR navigation - yes					1	2.9	0.0	10.8	0.1	7	05:30	5.4	5.4	16	0
fluorescence + CT navigation															
FGS + CT navigation	1			1		1.9	1.5	5.2	0.0	0	07:35	3.4	3.5	9	0
All others						2.9	0.0	9.8	0.1	7	05:04	6.4	6.1	18	0

Figure 1: (A) Schematic of gelatin phantom structure with 8 cm^3 cubical gelatin 'tumor' inclusion hidden within the cylindrical gelatin stroma. (B) Production batch of gelatin phantoms showing inclusion recesses into which tumor material will be injected; the lighter (pink) phantoms are fat-simulating, and the darker (red) phantoms are muscle-simulating. (C) Breakdown of the phantom groups in the study (90 total). (D) and (E) Demonstration of phantom dissection workflow in the operating room with undissected phantoms mounted on imaging platforms and imaging navigation technologies available. (F) Aggregated navigation modality performance.